PHYSICAL REVIEW C **88**, 011301(R) (2013)

Shell and isospin effects in nuclear charge radii

Ning Wang* and Tao Li
Department of Physics, Guangxi Normal University, Guilin 541004, People's Republic of China
(Received 6 May 2013; revised manuscript received 24 June 2013; published 17 July 2013)

The shell effect and isospin effect in nuclear charge radii are systematically investigated, and a four-parameter formula is proposed for the description of the root-mean-square (rms) charge radii by combining the shell corrections and deformations of nuclei obtained from the Weizsäcker-Skyrme mass model. The rms deviation with respect to the 885 measured charge radii falls to 0.022 fm. The proposed formula is also applied for the study of the charge radii of superheavy nuclei and nuclear symmetry energy. The linear relationship between the slope parameter L of the nuclear symmetry energy and the rms charge radius difference of the ^{30}S-^{30}Si mirror pair is clearly observed. The estimated slope parameter is about $L = 54 \pm 19$ MeV from the coefficient of the isospin term in the proposed charge radius formula.

DOI: 10.1103/PhysRevC.88.011301 PACS number(s): 21.10.Ft, 21.65.Ef, 21.10.Dr, 27.90.+b

As one of the basic nuclear properties, the root-mean-square (rms) charge radii of nuclei are of great importance for the study of nuclear structures [1,2] and nucleus-nucleus interaction potentials [3,4]. On one hand, the rms charge radii of nuclei can be self-consistently calculated by using microscopic nuclear mass models, such as the Skyrme-Hartree-Fock-Bogoliubov (HFB) model [5,6] and the relativistic mean-field (RMF) model [7,8]. The HFB21 model [6] can reproduce the 782 measured charge radii [9] with an rms deviation of 0.027 fm. On the other hand, the rms charge radii of nuclei are also frequently described by using mass- and isospin-dependent (or charge-dependent) phenomenological formulas [10–15]. Although these microscopic and phenomenological models can successfully describe the nuclear charge radii of most nuclei, the parabolic charge radii trend in the Ca isotope chain due to the shell closure of $N = 20$ and $N = 28$ cannot be reasonably well reproduced [2]. The shell effect directly influences the deformations of nuclei and, thus, affects the nuclear rms charge radii. To consider the shell effect, an empirical shell correction term, which is a function of the numbers of valence nucleons, was introduced in the phenomenological charge radius formulas [9,15] by assuming the proton magic numbers $Z_M =$ 2, 6, 14, 28, 50, 82, (114) and neutron magic numbers $N_M =$ 2, 8, 14, 28, 50, 82, 126, (184). Obviously, the fine structure of the nuclear charge radii for nuclei with semimagic numbers, such as $Z_M = 40, 64, 108$ and $N_M = 56, 162$ cannot be well described by the parametrized formulas. Microscopic shell corrections and the influence of nuclear deformations should be considered in the formula.

In addition to the shell effect, the isospin effect also plays a role for the nuclear charge radii. The nuclear symmetry energy, in particular, its density dependence, has received considerable attention in recent years [16–23]. The nuclear symmetry energy probes the isospin part of the nuclear force and intimately relates to the structure character of neutron-rich and neutron-deficient nuclei. The density dependence of the nuclear symmetry energy has been extensively investigated by using various models and experimental observables, such as the microscopic dynamics models [16,17], the nuclear mass models [6,15,24–26], the pygmy dipole resonance [27,28], the neutron star observations [21,29,30], and so on. In particular, the neutron skin thickness of ^{208}Pb is found to be a sensitive observable to constrain the slope parameter L of the nuclear symmetry energy at the saturation density since the linear relationship between the slope parameter L and the neutron skin thickness $\Delta R_{\rm np}$ of ^{208}Pb was clearly observed [20,31]. However, it is difficult to precisely measure the neutron radius of ^{208}Pb in experiments, which results in a large uncertainty of the extracted slope parameter. By comparing with the neutron radii of the nuclei, the rms charge radii of the nuclei can be measured with relatively high accuracy. It would be helpful if the slope parameter could be determined from the charge radii of the nuclei. It is known that, in the absence of Coulomb interactions between the protons, a perfectly charge-symmetric and charge-independent nuclear force would result in the binding energies of mirror nuclei (i.e., nuclei with the same atomic number A but with the proton number Z and neutron number N interchanged) being identical [32,33]. In this case, the neutron skin thickness of a neutron-rich nucleus approximately equals the proton radius difference (in absolute value) of this nucleus and its mirror partner. It is, therefore, interesting to investigate the correlation between the charge radius difference of the mirror nuclei and the slope parameter L of the nuclear symmetry energy.

In this Rapid Communication, we attempt to propose a phenomenological formula for the global description of the nuclear rms charge radii by combining the deformations and shell corrections of nuclei obtained from the Weizsäcker-Skyrme (WS*) mass model [24,25], which is based on the macroscopic-microscopic method together with the Skyrme energy-density functional and mirror constraint from the isospin symmetry.

Based on the consideration of the nuclear saturation property, the nuclear charge radius R_c is usually described by the $A^{1/3}$ law: $R_c = r_0 A^{1/3}$, where A is the mass number. By considering the quadrupole β_2 and the hexadecapole β_4 deformations of the nuclei, the rms charge radius $r_{\rm ch}$ of a

*wangning@gxnu.edu.cn

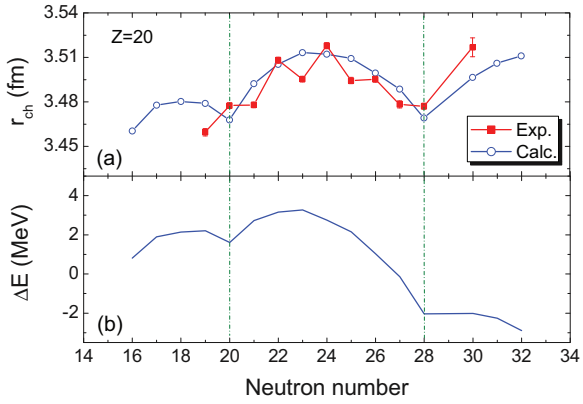

FIG. 1. (Color online) (a) Nuclear rms charge radii of Ca isotopes [35]. (b) Shell corrections of Ca isotopes obtained from the WS* mass model [25]. The open circles in (a) denote the calculated results in this Rapid Communication with Eqs. (1) and (2).

nucleus can be approximately written as [11]

$$r_{\rm ch} = \langle r^2 \rangle^{1/2} \simeq \sqrt{\frac{3}{5}} R_c \left[1 + \frac{5}{8\pi} \left(\beta_2^2 + \beta_4^2 \right) \right]. \qquad (1)$$

For a better description of the charge radii of light nuclei and nuclei far from the β-stability line, the mass- and isospin-dependent radius coefficient r_0 was introduced [10], i.e., $R_c = r_0 A^{1/3}(1 + \kappa/A - \alpha I)$ with the isospin asymmetry $I = (N - Z)/A$. In addition to the mass and isospin dependence of the nuclear charge radii, it is found that the shell effect also plays a role for some nuclei [15]. In Fig. 1, we show the rms charge radii of Ca isotopes and the corresponding shell corrections of nuclei from the WS* mass model [25]. One sees that the parabolic trend of the rms charge radii of Ca isotopes between $N = 20$ and 28 seems to be consistent with that of the corresponding shell corrections, which implies that to consider the shell effect could be helpful for a better description of the nuclear charge radii.

By considering the influence of the shell effect in nuclei, we propose a modified four-parameter formula for the description of the nuclear charge radius R_c,

$$R_c = r_0 A^{1/3} + r_1 A^{-2/3} + r_s I(1 - I) + r_d \Delta E/A, \qquad (2)$$

where ΔE denotes the shell corrections of the nuclei from the WS* mass model with which the 2149 known masses in AME2003 [34] can be reproduced with an rms deviation of 441 keV and the shell gaps for the magic nuclei can also be well reproduced. The r_s term in Eq. (2), which is different from the isospin term in the available phenomenological radius formulas, will be discussed later. Based on the 885 measured rms charge radii for nuclei [35] with $A \geqslant 16$ together with the deformations β_2, β_4 and shell corrections ΔE of nuclei obtained from the WS* mass model [25] and searching for the minimal rms deviation

$$\sigma^2 = \frac{1}{m} \sum \left(r_{\rm ch}^{\rm exp} - r_{\rm ch}^{\rm th} \right)^2, \qquad (3)$$

between the experimental data and model calculations, we obtain the optimal values for the four parameters which are listed in Table I. By comparing with the rms deviation between the 885 measured radii and the HFB21 calculations [6], which is 0.026 fm, the corresponding result in this Rapid Communication falls to 0.022 fm. With the microscopic shell corrections, the rms deviation in the charge radii can be reduced by 17%. From Fig. 1(a), one sees that the known rms charge radii of the Ca isotopes can be reproduced reasonably well.

TABLE I. Parameters of the charge radius formula R_c and the rms deviation σ with respect to the 885 measured rms charge radii [35]. The unit for r_d is MeV^{-1} fm, and those for the others are femtometers.

r_0	r_1	r_s	r_d	σ
1.2260(9)	2.86(9)	−1.09(3)	0.99(17)	0.022

For the isospin term in the charge radius formulas, the forms I^2, $IA^{1/3}$, and $(I - I_0)A^{1/3}$ were proposed in Ref. [15], Ref. [10] and Ref. [9], respectively. Here, $I_0 \simeq 0.4A/(A + 200)$ denotes the corresponding isospin asymmetry of nuclei along the β-stability line. We note that the rms deviation can be further reduced by about 15% with a new form $I(1 - I)$ by comparing with the result that uses the form $IA^{1/3}$. In Fig. 2, we show the isospin dependence of the relative rms charge radii. Here the relative rms charge radius of a nucleus is given by $\delta r_{\rm ch} = r_{\rm ch}^{\rm exp} - \sqrt{\frac{3}{5}}(r_0 A^{1/3} + r_1 A^{-2/3} + r_d \Delta E/A)$ without considering the influence of nuclear deformations. By comparing with the linear form, the form $I(1 - I)$ gives relatively better results for the extremely neutron-rich nuclei since the decreasing trend of the charge radii gradually weakens with the increase in isospin asymmetry. We also note that the value of nuclear radius constant r_0 in Eq. (2), which relates to the saturation properties of symmetric nuclear matter and neutron matter, is very close to the value (1.2257 fm) proposed in Ref. [36].

Based on the proposed four-parameter nuclear charge radius formula, the known experimental data are systematically investigated. In Fig. 3, we show the difference between the experimental data and the model calculations for the 885 rms charge radii of the nuclei. From the results of the two quite different models, one sees that the trends in the differences are similar to each other, which is due to the fact that the

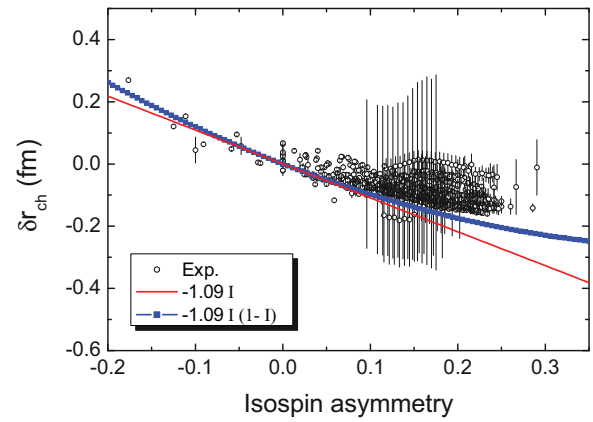

FIG. 2. (Color online) Relative rms charge radii of nuclei as a function of isospin asymmetry I.

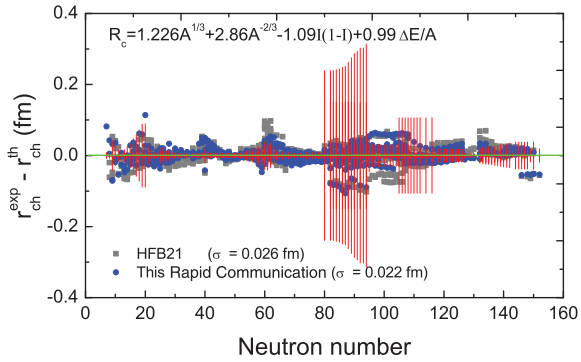

FIG. 3. (Color online) Difference between the experimental data and the model calculations for the 885 rms charge radii of nuclei [35]. The squares and solid circles denote the results of the HFB21 model and those in this Rapid Communication, respectively. The error bars denote the uncertainty of the experimental data.

obtained deformations of the nuclei with the HFB21 mass model are comparable with the results from the WS* mass model. The calculated rms deviation with the proposed formula is only 0.022 fm, which is smaller than the results of the HFB21 model by 15%. Here, we also present the results of the microscopic RMF model in Fig. 4 for comparison. In Ref. [7], the rms charge radii of even-even nuclei with $Z \geqslant 10$ are systematically calculated by using the RMF model with the force NL3. For the measured rms charge radii of 343 even-even nuclei, the rms deviation with the proposed formula is 0.016 fm, which is significantly smaller than the result (0.026 fm) of the RMF calculations. For nuclei with charge numbers $Z < 20$ and $Z \approx 78$, the results of the proposed formula are better than those of the RMF calculations. It is partly due to the fact that the shell corrections and the deformations for the nuclei with the new magic numbers, such as $N = 14$, 16 and for the nuclei with the subshell closure are reasonably well described by the WS* mass model.

In Fig. 5, we show the comparisons of the rms charge radii for Ca, Ni, Zr, and Pb isotopes from three models. For the Ca isotopes, neither the HFB21 model nor the RMF

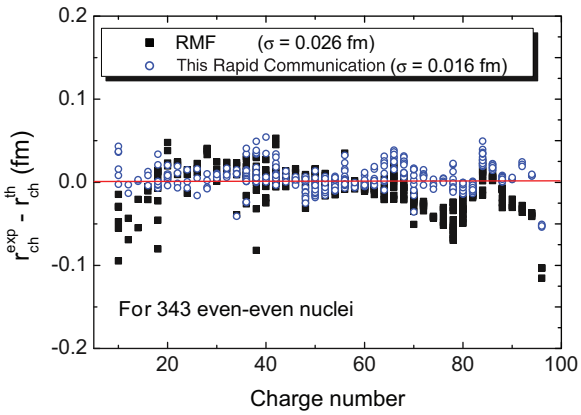

FIG. 4. (Color online) Difference between the experimental data and the model calculations for the rms charge radii of 343 even-even nuclei [35]. The squares and circles denote the results of the RMF model [7] and those in this Rapid Communication, respectively.

model reproduce the trend of the experimental data. For the Ni isotopes, the experimental data are systematically overpredicted by the HFB21 model and are underpredicted by the RMF model. For the doubly magic nucleus ^{56}Ni, the calculated quadrupole deformation of the nucleus is $\beta_2 = 0.16$ with the HFB21 model. For other Ni isotopes, the obtained β_2 values from the HFB21 calculations are significantly larger than the results of WS*, which results in the overpredicted results for the Ni isotopes. According to the RMF calculations, we note that the binding energies of ^{58,60,62,64}Ni are systematically underpredicted by about 4 MeV, which might affect the reliable description of the rms charge radii. For the Zr isotopes, one sees that the rms charge radii for nuclei with $N = 50$, 56, and 58 can be remarkably well reproduced with the proposed formula since the shell corrections and deformations of these nuclei (with shell or subshell closure) are reasonably well described by the WS* mass model. For the neutron-deficient Pb isotopes, the rms charge radii are significantly overpredicted by the HFB21 calculations, and the kink at $N = 126$ cannot be reproduced. The global trend of the rms charge radii for the nuclei in Fig. 5, especially the kinks at the magic numbers, can be well described by using the proposed nuclear charge radius formula.

In Fig. 6, we show the predicted rms charge radii with the proposed formula for some superheavy nuclei. The solid curve denotes the results of the HFB21 model for Hs ($Z = 108$) isotopes, which are comparable with the predictions of this Rapid Communication (the deviations are smaller than 0.05 fm in general). For the superheavy nuclei ^{286}114 and ^{290}116, the extracted rms charge radii from the experimental α-decay data are $r_{\rm ch} = 6.24 \pm 0.14$ and 6.13 ± 0.16 fm [37], respectively. The predicted results in this Rapid Communication for these two nuclei are 6.17 and 6.19 fm, respectively, which are comparable with the extracted results in Ref. [37].

In this Rapid Communication, we simultaneously investigate the correlation between the nuclear symmetry energy and the isospin term of the charge radius formula. We study the difference in the rms charge radii between mirror nuclei, such as the ^{30}S-^{30}Si pair. Because of the influence of the new magic numbers $N = 14$, 16, the calculated deformations of these two nuclei are very small with some different mass models, such as the Weizsäcker-Skyrme mass model, the finite range droplet model [38], and the HFB calculations [5], which adopt three widely used Skyrme forces SLy4, SkP, and SkM*. We systematically calculate the difference in the rms charge radii $\Delta r_{\rm ch}$ between ^{30}S and ^{30}Si by using the Skyrme-Hartree-Fock model with 62 different Skyrme forces in which the corresponding incompressibility coefficient for the symmetry nuclear matter is $K_\infty = 210$–280 MeV and the saturation density is $\rho_0 = 0.15$–0.17 fm^{-3}. From Fig. 7, one can clearly see the linear relationship between the slope parameter L and the difference in the rms charge radii $\Delta r_{\rm ch}$. The Pearson (linear) correlation coefficient r of L with $\Delta r_{\rm ch}$ for the 62 Skyrme forces is 0.95, which is comparable with the corresponding value (0.97) of L with the neutron skin thickness of ^{208}Pb for the same forces. The values of $\Delta r_{\rm ch}$ for measured mirror pairs, such as ^{34}S-^{34}Ar and ^{18}O-^{18}Ne are also investigated with the deformed configurational Skyrme-Hartree-Fock calculations [39]. We note that the obtained linear correlation coefficients

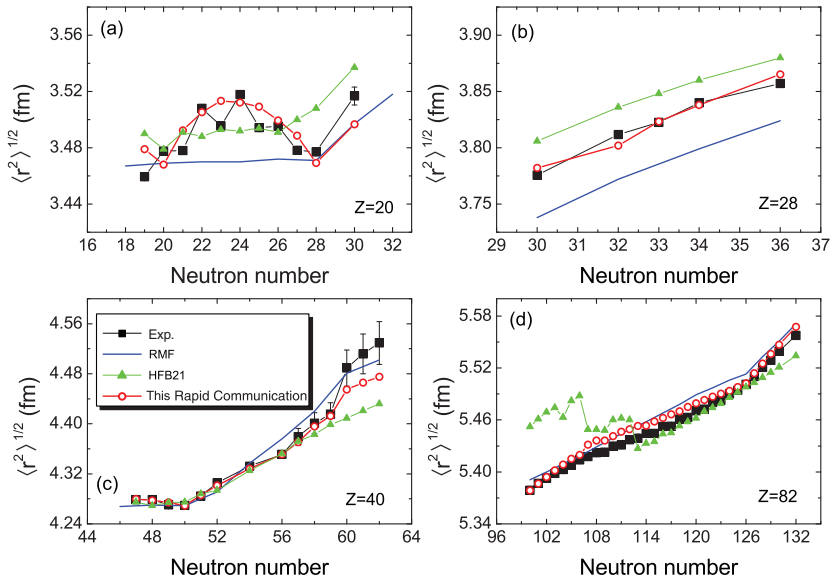

FIG. 5. (Color online) Comparisons of the rms charge radii for Ca, Ni, Zr, and Pb isotopes. The triangles, solid curves, and solid squares denote the results of the HFB21, RMF, and experimental data, respectively. The open circles denote the results in this Rapid Communication according to Eqs. (1) and (2).

r for these two pairs are 0.58 and 0.69, respectively, which are significantly smaller than the value for the mirror pair ^{30}S-^{30}Si. It indicates that the linear relationship between L and $\Delta r_{\rm ch}$ for the two pairs ^{34}S-^{34}Ar and ^{18}O-^{18}Ne are not as good as that for the mirror pair ^{30}S-^{30}Si due to the influence of the new magic numbers $N = 14, 16$. By considering the fact that the experimental uncertainty for the rms charge radius measurement is much smaller than that for the rms neutron radius, precise measurements of the rms charge radii for the pair of mirror nuclei ^{30}S-^{30}Si, especially the unmeasured ^{30}S, could be very helpful for the extraction of the slope parameter.

Due to the perfectly charge-symmetric and charge-independent nuclear force, the deformations and shell correction of a nucleus approximately equal those of its mirror nucleus [25,40]. Based on the proposed nuclear charge radius formula, one obtains $\Delta r_{\rm ch} \approx \sqrt{\frac{3}{5}} 2 r_s I$ by neglecting the influence of the nuclear deformations. For the ^{30}S-^{30}Si mirror pair, the estimated value of $\Delta r_{\rm ch}$ is about 0.113 ± 0.003 fm, and the corresponding slope parameter is about $L = 54 \pm 19$ MeV, which is consistent with the recently extracted results from the Fermi-energy difference in nuclei [41] and from modeling x-ray bursts and quiescent low-mass x-ray binaries [42,43]. In addition, the extracted slope parameter $L = 52.5 \pm 20$ MeV from the Skyrme-Hartree-Fock calculations together with the neutron skin thickness of Sn isotopes [44] and $L = 52.7 \pm 22.5$ MeV from the global nucleon optical potentials [45] are in good agreement with the estimated result in this Rapid Communication.

To summarize, by combining the Weizsäcker-Skyrme mass model, we propose a four-parameter nuclear charge radius formula in which the microscopic shell correction and nonlinear isospin terms are introduced. The 885 measured

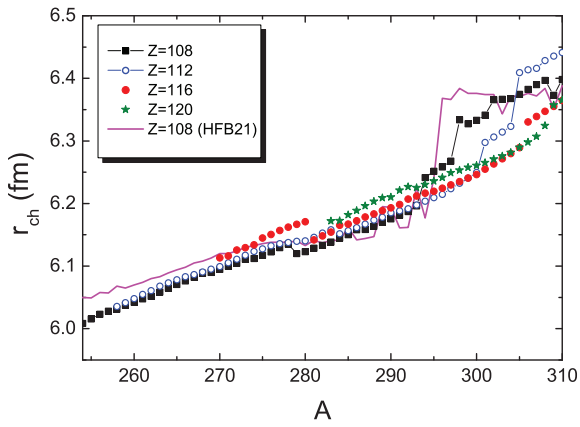

FIG. 6. (Color online) Predicted rms charge radii with the proposed formula for some superheavy nuclei. The solid curve denotes the results of the HFB21 model for Hs ($Z = 108$) isotopes.

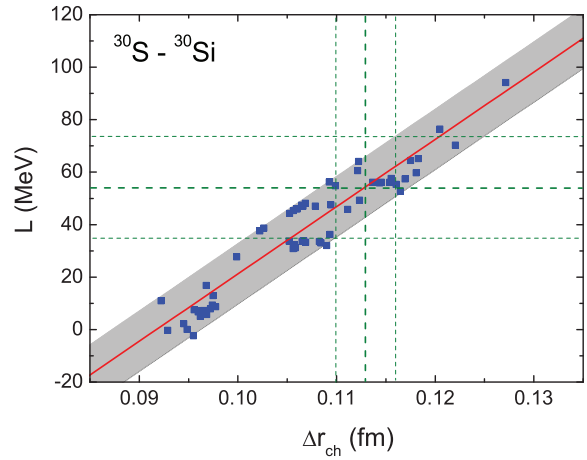

FIG. 7. (Color online) Slope parameter of the nuclear symmetry energy as a function of the rms charge radius difference between ^{30}S and ^{30}Si. The squares denote the calculated results by using the Skyrme-Hartree-Fock model with 62 different Skyrme forces. The solid line with shadows is a linear fit to the squares. The dashed horizontal lines denote the estimated slope parameter according to the r_s value of the proposed charge radius formula.

rms charge radii of the nuclei are reproduced with an rms deviation of 0.022 fm. For the measured even-even nuclei, the rms deviation is only 0.016 fm. The parabolic charge radii trend in the Ca chain due to the shell effect and the trend of Ni, Zr, and Pb isotopes are reasonably well described with the formula. Through a study of the difference in the rms charge radii $\Delta r_{\rm ch}$ between mirror nuclei by using the Skyrme-Hartree-Fock model with 62 different Skyrme forces, the linear relationship between slope parameter L and $\Delta r_{\rm ch}$ for the mirror pair ^{30}S-^{30}Si is clearly observed, which would be helpful for the extraction of the slope parameter of the nuclear symmetry energy. The estimated slope parameter from the coefficient r_s of the isospin term in the proposed formula is about $L = 54 \pm 19$ MeV.

This work was supported by the National Natural Science Foundation of China Grant No. 11275052.

[1] I. Angeli, Y. P. Gangrsky, K. P. Marinova, I. N. Boboshin, S. Y. Komarov, B. S. Ishkhanov, and V. V. Varlamov, J. Phys. G **36**, 085102 (2009).
[2] Y. P. Gangrsky, K. P. Marinova, S. G. Zemlyanoi, I. D. Moore, J. Billowes, P. Campbell, K. T. Flanagan, D. H. Forest, J. A. R. Griffith, J. Huikari *et al.*, J. Phys. G **30**, 1089 (2004).
[3] W. Reisdorf, J. Phys. G **20**, 1297 (1994).
[4] J. M. Wang, H. F. Zhang, and J. Q. Li, J. Phys. G **40**, 045103 (2013).
[5] M. V. Stoitsov, J. Dobaczewski, W. Nazarewicz, S. Pittel, and D. J. Dean, Phys. Rev. C **68**, 054312 (2003), and references therein.
[6] S. Goriely, N. Chamel, and J. M. Pearson, Phys. Rev. C **82**, 035804 (2010); http://www-astro.ulb.ac.be/bruslib/nucdata/hfb21-dat
[7] G. A. Lalazissis, S. Raman, and P. Ring, At. Data Nucl. Data Tables **71**, 1 (1999).
[8] P. W. Zhao, Z. P. Li, J. M. Yao, and J. Meng, Phys. Rev. C **82**, 054319 (2010).
[9] I. Angeli, At. Data Nucl. Data Tables **87**, 185 (2004).
[10] B. Nerlo-Pomorska and K. Pomorski, Z. Phys. A **348**, 169 (1994).
[11] S. Q. Zhang, J. Meng, S.-G. Zhou, and J. Y. Zeng, Eur. Phys. J. A **13**, 285 (2002).
[12] J. Piekarewicz, M. Centelles, X. Roca-Maza, and X. Viñas, Eur. Phys. J. A **46**, 379 (2010).
[13] Y. A. Lei, Z. H. Zhang, and J. Y. Zeng, Commun. Theor. Phys. **51**, 123 (2009).
[14] J. Duflo, Nucl. Phys. A **576**, 29 (1994).
[15] A. E. L. Dieperink and P. Van Isacker, Eur. Phys. J. A **42**, 269 (2009).
[16] M. B. Tsang, Y. X. Zhang, P. Danielewicz, M. Famiano, Z. Li, W. G. Lynch, and A. W. Steiner, Phys. Rev. Lett. **102**, 122701 (2009).
[17] L. W. Chen, C. M. Ko, and B. A. Li, Phys. Rev. Lett. **94**, 032701 (2005).
[18] D. V. Shetty, S. J. Yennello, and G. A. Souliotis, Phys. Rev. C **76**, 024606 (2007).
[19] A. S. Botvina, O. V. Lozhkin, and W. Trautmann, Phys. Rev. C **65**, 044610 (2002).
[20] M. Centelles, X. Roca-Maza, X. Viñas, and M. Warda, Phys. Rev. Lett. **102**, 122502 (2009).
[21] A. W. Steiner and S. Gandolfi, Phys. Rev. Lett. **108**, 081102 (2012).
[22] A. W. Steiner, M. Prakash, J. M. Lattimer, and P. J. Ellis, Phys. Rep. **411**, 325 (2005).
[23] J. Dong, W. Zuo, and W. Scheid, Phys. Rev. Lett. **107**, 012501 (2011).
[24] N. Wang, M. Liu, and X. Wu, Phys. Rev. C **81**, 044322 (2010); http://www.imqmd.com/mass/
[25] N. Wang, Z. Liang, M. Liu, and X. Wu, Phys. Rev. C **82**, 044304 (2010); http://www.imqmd.com/mass/WS3.3.txt
[26] M. Liu, N. Wang, Z. X. Li, and F. S. Zhang, Phys. Rev. C **82**, 064306 (2010).
[27] A. Klimkiewicz, N. Paar, P. Adrich, M. Fallot, K. Boretzky, T. Aumann, D. Cortina-Gil, U. Datta Pramanik, T. W. Elze, H. Emling *et al.*, Phys. Rev. C **76**, 051603 (2007).
[28] A. Carbone, G. Colò, A. Bracco, L. G. Cao, P. F. Bortignon, F. Camera, and O. Wieland, Phys. Rev. C **81**, 041301(R) (2010).
[29] D.-H. Wen, W. G. Newton, and B.-A. Li, Phys. Rev. C **85**, 025801 (2012).
[30] J. M. Lattimer, Annu. Rev. Nucl. Part. Sci. **62**, 485 (2012).
[31] X. Roca-Maza, M. Centelles, X. Viñas, and M. Warda, Phys. Rev. Lett. **106**, 252501 (2011).
[32] S. M. Lenzi and M. A. Bentley, Lect. Notes Phys. **764**, 57 (2009).
[33] S. Shlomo, Rep. Prog. Phys. **41**, 957 (1978).
[34] G. Audi, A. H. Wapstra, and C. Thibault, Nucl. Phys. A **729**, 337 (2003).
[35] I. Angeli and K. P. Marinova, At. Data Nucl. Data Tables **99**, 69 (2013).
[36] G. Royer and R. Rousseau, Eur. Phys. J. A **42**, 541 (2009).
[37] D. Ni, Z. Ren, T. Dong, and Y. Qian, Phys. Rev. C **87**, 024310 (2013).
[38] P. Möller, J. R. Nix *et al.*, At. Data Nucl. Data Tables **59**, 185 (1995).
[39] M. V. Stoitsov, J. Dobaczewski, W. Nazarewicz, and P. Ring, Comput. Phys. Commun. **167**, 43 (2005).
[40] K. Setoodehnia, A. A. Chen, D. Kahl, T. Komatsubara, J. José, R. Longland, Y. Abe, D. N. Binh, J. Chen, S. Cherubini *et al.*, Phys. Rev. C **87**, 065801 (2013).
[41] N. Wang, L. Ou, and M. Liu, Phys. Rev. C **87**, 034327 (2013).
[42] A. W. Steiner, J. M. Lattimer, and E. F. Brown, Astrophys. J. **722**, 33 (2010).
[43] K. Hebeler, J. M. Lattimer, C. J. Pethick, and A. Schwenk, arXiv:1303.4662.
[44] L.-W. Chen, Phys. Rev. C **83**, 044308 (2011).
[45] C. Xu, B.-A. Li, and L.-W. Chen, Phys. Rev. C **82**, 054607 (2010).